Journal of Innovative Image Processing (ISSN: 2582-4252)
www.irojournals.com/iroiip/

Entropy-Guided Feature Fusion Deep Learning Framework for Orange Fruit Disease Detection

Mahalakshmi C.[1*], Saravanan S.[2]

[1]Research Scholar, Department of Computer and Information Science, Annamalai University, Annamalai Nagar, Chidambaram, India.
[2]Assistant Professor, Department of Computer and Information Science, Faculty of Science, Annamalai University, Annamalai Nagar, Chidambaram, India.

E-mail: [1*]mahabharathi3219@gmail.com, [2]aucissaran@gmail.com

Orcid ID: [1*]0009-0004-2591-2660, [2]0000-0001-6494-8798

Abstract

Automated detection and classification of orange diseases will greatly help to save money on fruit deterioration, improve fruit quality, and provide for long-term orange sustainability. Orange diseases usually appear as surface lesions or discoloration and can decrease the market price of the fruit and the likelihood of post-harvest decay. Since current inspection techniques depend heavily on the manual observations of trained inspectors, they are inefficient, biased, and cannot be applied to commercial-scale operations. Therefore, to address these issues, an automatic disease detection and classification framework using a Deep Convolutional Recurrent Neural Network (DCRNN) enabled by the optimization process of an Enhanced Sea Horse Optimization (ESHO) algorithm is developed. Pre-processing images with a Wiener filter to remove noise, CLAHE to amplify image contrast, and color-based segmentation to distinguish areas affected by disease via RGB thresholding is implemented. Next, deep feature extraction is achieved utilizing multiple pretrained convolutional models (i.e., ResNet50, VGG-16, and NasNet), which have different properties and are combined into one model using an entropy-based fusion technique. To achieve better performance by adjusting the hyperparameters of the DCRNN model, an Enhanced Sea Horse Optimization (ESHO) algorithm is utilized. Finally, classification of the disease is achieved using sophisticated machine learning algorithms such as SSAE, MHA-LSTM, and DCRNN. Additionally, Grad-CAM visualization was employed to enhance model interpretability by highlighting the disease-affected regions that influenced the classification decisions. Experiments were conducted using an open-source dataset for orange fruits, demonstrating that proposed ESHO-DCRNN framework produces better results than the traditional deep neural network approaches for detecting orange diseases, reaching 99.50% accuracy.

Keywords: Entropy-Guided Feature Fusion, Enhanced Sea Horse Optimization (ESHO), VGG-16, Deep Convolutional Recurrent Neural Network (DCRNN), Orange Fruit Disease Detection.

*** Corresponding Author**

DOI: https://doi.org/10.36548/jiip.2026.3.022
Received: 21.05.2026, received in revised form: 25.06.2026, accepted: 14.07.2026, published: 23.07.2026
© 2026 Inventive Research Organization. This is an open access article under the Creative Commons Attribution-NonCommercial International (CC BY-NC 4.0) License

1. Introduction

Orange cultivation is the world's largest orange production industry, owing to the high nutritional content and flavor of oranges, which also contribute significantly to the global agricultural economy [1]. As a great source of vitamin C, nutritional fiber, and antioxidants, oranges are a significant part of human nutrition and food security. By reason of the widespread farming and economic significance of oranges, maintaining the quality and health of orange fruits is a necessity to ensure the long-term sustainability of agriculture and to minimize the economic impact of potential crop failures. Nonetheless, many of the numerous diseases affecting orange production present as visible lesions, discoloration, and/or surface deformity, reducing both the marketability and the shelf-life of orange fruits [2]. Thus, it is crucial to detect the diseases of orange fruits at an early phase of development and with an acceptable degree of accuracy so that both yield loss can be minimized and disease control measures can be taken in a timely manner. Traditional methods of diagnosing diseases include manually inspecting crops by experienced growers or agricultural professionals. While these traditional methods are somewhat effective, they are typically time-consuming, expensive, and subjective, resulting in variable levels of success depending upon factors such as the individual performing the inspections, the size of the area being inspected, and the presence of trained personnel in the region [3]. This creates a need for automated, scalable disease detection systems that offer constant and objective support to growers.

In recent years, Deep Learning (DL) models have greatly improved the detection of diseases in crops through image analysis [4]. Mainly, Convolutional Neural Networks (CNNs) have shown great promise for recognizing spatial features of plants and fruits that differentiate healthy from diseased plants and fruits [5]. However, while CNNs show great potential for disease detection, they typically do not take advantage of temporal dependencies and contextual relationships within the features extracted from the images. Furthermore, relying solely on a single feature extractor or classifier limits the model's performance across diverse environmental conditions. The increasing demand for accurate and early detection of orange fruit diseases has created a strong need for smart automated systems that could minimize dependency on manual inspection. The traditional approach frequently struggles with variability in illumination, intricate backgrounds, and subtle disease patterns, leading to inconsistent performance in real-world conditions. These challenges emphasize the necessity for a stronger, adaptive, and high-accuracy model that can efficiently learn discriminative disease features from fruit images. To address these limitations, this study introduces an Efficient Feature-Fusion and Optimization-Based Deep Learning Model for Orange Fruit Disease Detection and Classification. The major contributions of this study are as follows:

- A hybrid deep learning model that combines CNN-based feature extraction with recurrent learning for orange disease classification.
- An entropy-driven feature fusion strategy for combining multi-CNN representations into a compact discriminative feature vector.
- An Enhanced Sea Horse Optimization (ESHO) algorithm for automatic hyperparameter tuning of the DCRNN model.
- A DCRNN architecture capable of capturing both spatial and sequential dependencies in fused feature space.
- A Grad-CAM visualization is applied to improve the model interpretability.

- Comprehensive evaluation against advanced models demonstrating superior performance (99.50% accuracy).

The remainder of the paper is structured as follows: Section 2 explains an overview of relevant literature in the field; Section 3 outlines the proposed methodology in greater detail; Section 4 discusses the experimental results obtained and evaluates the performance of the proposed methodology; and Section 5 concludes the study with key findings and future research directions.

2. Related Works

Kumar et. al., [6] utilized Machine Learning models to classify multiclass orange diseases. Specifically, it demonstrated that the CNN model utilizing MobileNetV2 architecture was able to identify four diseases of oranges (Blackspot, Canker, Fresh, and Greening) with an accuracy level of 98.22%. Thomse et al., [7] employed Artificial Intelligence (AI) and Convolutional Neural Network (CNN) architectures such as VGG-16 to detect and classify orange disease and nutrient shortages in orange leaves, achieving 87% accuracy on a large dataset of healthy versus diseased leaves. Sghir et al., [8] presented a data-driven method for detecting and classifying diseases in oranges. This was done by using pre-trained CNN models to analyze a large dataset of orange images. Results indicated that CNN-based approaches resulted in 92.17% accuracy, and ResNet-50-based approaches resulted in 97.28% accuracy when analyzing 1,790 images of oranges that were either fresh or had one of three disease types.

Suryavanshi et al., [9] proposed a method to detect and classify citrus greening disease in oranges by employing a combination of CNN, random forests (RF), and image analysis of orange leaves that are disease-free and those that have been infected. High levels of accuracy were realized due to the ability to distinguish between disease-free and sick orange leaves via image analysis. Chauhan [10] used a MobileNetV2 classification model to identify and categorize diseases of oranges; it achieved a high accuracy rate of 95% in differentiating healthy oranges from those with disease, and thus enhances early identification and protection of crops. Kaur et al., [11] introduced "DeepCitrus," a hybrid model that combines CNN and VGG16 architectures to automatically recognize and categorize orange leaf diseases. Yadav et al., [12] showed customized shallow CNN and RBF SVM with higher accuracy when classifying 'Valencia' orange fruit surface with citrus black spot and four other diseases, thus, showing that automated disease recognition and classification are achievable through effective methods. Kalaivani and Sathya., [13] demonstrated that a hybrid CNN is utilized for disease classification and k-means clustering for disease image segmentation, demonstrating a 99.2% classification accuracy for recognizing and classifying orange fruit disease. Behera et al., [14] presented a computer vision-based method to recognize and classify orange fruit disease through multi-class SVM and k-means clustering. In addition, they use fuzzy logic to evaluate the severity of the diseases and subsequently apply pesticides effectively.

Although previous studies have reported promising performance in orange disease classification using deep learning and machine learning techniques, most of them rely on a single feature extraction model, such as MobileNetV2, VGG16, or ResNet50, which may limit the diversity of learned feature representations. In addition, many existing approaches primarily focus on improving classification accuracy without incorporating effective feature fusion strategies, advanced hyperparameter optimization techniques, or model interpretability. Furthermore, only a few studies integrate explainable artificial intelligence (XAI) to provide visual justification for the model's predictions. Therefore, there is a research gap in developing a unified framework that combines complementary feature extraction from multiple deep learning models, entropy-based feature fusion, optimized multiclass classification, and explainability. To address this gap, the proposed framework integrates ResNet50, VGG-16, and NASNet for feature extraction, entropy-based feature fusion, ESHO-based hyperparameter optimization for multiple classifiers, and Grad-CAM to provide accurate and interpretable orange disease classification.

3. Proposed Work

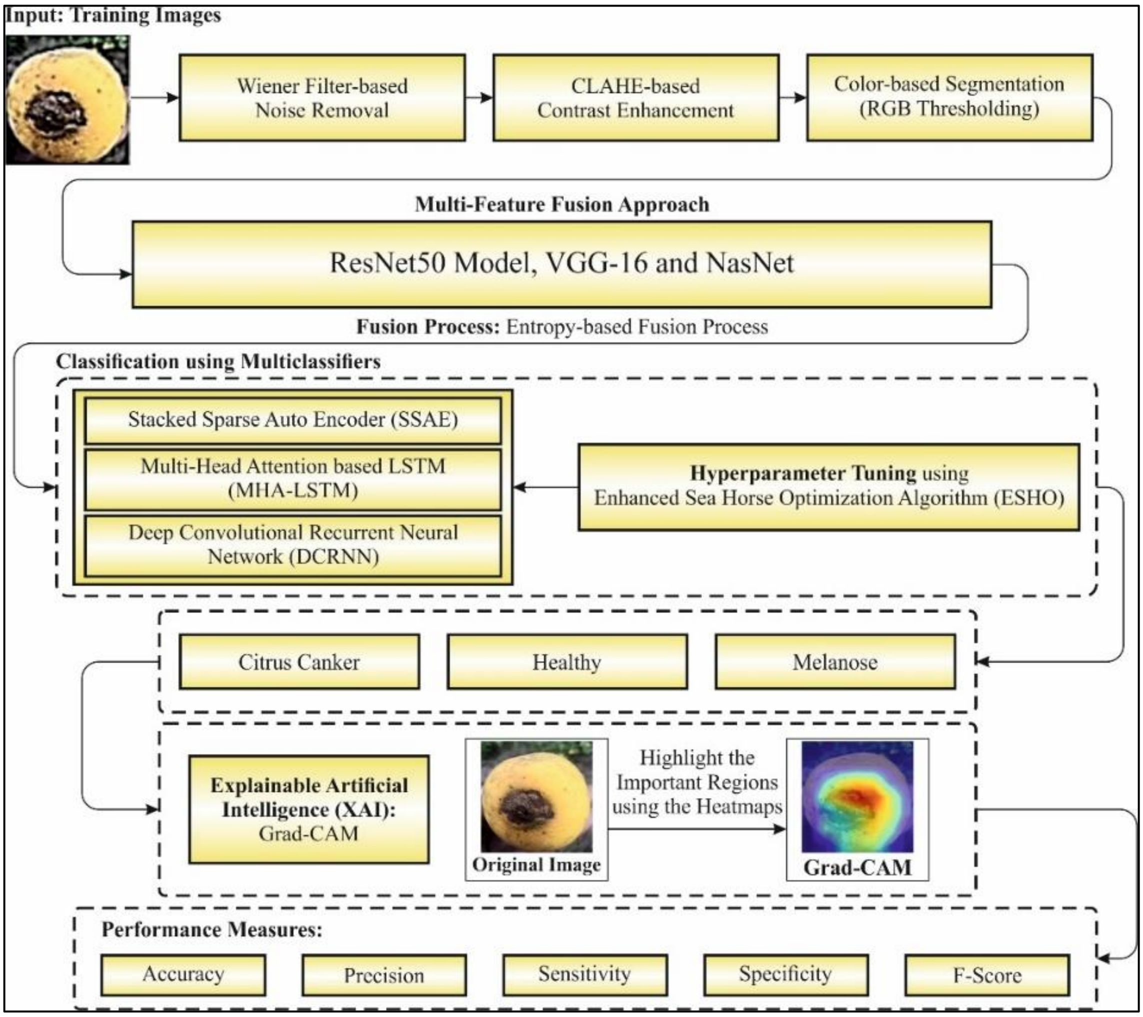

Figure 1. Workflow of the proposed ESHO-DCRNN technique

The ESHO-DCRNN approach to orange fruit disease image classification uses a structured image processing pipeline, as shown in Figure 1. The process begins with a Wiener-filter-based denoising step that efficiently removes noise from the orange fruit images, keeping the important surface texture information and disease-related details, thus preparing the images for later use. Following denoising, CLAHE is used to increase local contrast and make disease symptoms like lesions, discoloration, and surface anomalies visible. Then, color-based segmentation using RGB thresholding isolates the diseased area from the healthy area of the orange fruit to eliminate background interference and concentrate on specific pathological features. Afterward, in the segmentation stage, different pre-trained CNN frameworks—

namely ResNet50, VGG-16, and NasNet—are utilized for deep feature extraction from the segmented images. These deep features contain complementary and discriminative spatial representations of the disease characteristics. The extracted features are then fused into a compact and informative feature set using an entropy-based fusion strategy. Finally, the ESHO method optimizes the hyperparameters of the DCRNN model, which helps obtain the best model configuration and improves model convergence. The optimized feature representation is then classified by advanced learning models like SSAE, MHA-LSTM, and DCRNN. Among these, the DCRNN can capture both the spatial and sequential dependency of the fused feature space and therefore accurately classify orange fruit diseases into multi-class categories. Furthermore, Grad-CAM visualization is used to improve model interpretability by highlighting the disease-affected regions that influenced the classification decisions. A detailed description of each processing step—comprising pre-processing, segmentation, feature fusion, feature extraction optimization, and classification—is presented in the subsequent sections, and the pseudocode is given in Algorithm 1.

Algorithm 1: Pseudocode of proposed ESHO-DCRNN framework

Input: Orange fruit image dataset (I)
Output: Disease class label (C) and Grad-CAM visualization map (G)
Step 1: Dataset Collection
Step 2: Preprocess the input images:

- Apply Wiener filtering to remove noise.
- Apply CLAHE for contrast enhancement.
- Resize and normalize images.

Step 3: Segment preprocessed images:

- Apply RGB thresholding to identify disease-affected regions.
- Generate segmented disease masks.

Step 4: Derive deep features using DL models:

- Extract features using ResNet50.
- Extract features using VGG16.
- Extract features using NasNet.

Step 5: Employ entropy-based feature fusion to integrate the derived features into a unified representation.
Step 6: Initialize ESHO parameters, including population size (N), maximum iterations (T), and hyperparameter search space (H).
Step 7: Apply ESHO-based hyperparameter optimization:

- Generate candidate hyperparameter solutions.
- Evaluate classifier performance using each candidate solution.
- Update candidate solutions using exploration and exploitation strategies.
- Identify and retain the best hyperparameter set (H_{best}).

Step 8: Train SSAE, MHA-LSTM, and DCRNN classifiers using the fused features and optimized hyperparameters.
Step 9: Select the classifier with the best validation performance for disease prediction.
Step 10: Generate disease class labels for the test samples.
Step 11: Apply Grad-CAM to visualize the disease regions contributing to the classification decision.
Step 12: Compute evaluation metrics including accuracy, precision, recall, F1-score, and AUC.
Step 13: Return the predicted disease class and Grad-CAM visualization

3.1 Wiener Filter – Based Noise Removal

Wiener filters are an excellent tool for restoring images impacted by additive noise and blur, with a wide variety of applications in image restoration and noise removal. Orange fruit images acquired in a natural or semi-controlled environment typically contain various types of noise due to varying light, sensor constraints, and environmental issues. The Wiener filter (WF) can be used to remove these forms of noise by reducing the difference between the actual and the cleaned-up images, thus providing clearer images before further disease analysis is done, as shown in Figure 2. The Wiener filter is expressed as follows:

$$\hat{\mathrm{I}}(\mathrm{a},\mathrm{b}) = \frac{\mathrm{H}*(\mathrm{a},\mathrm{b})}{|\mathrm{H}(\mathrm{a},\mathrm{b})|^2 + \frac{\mathrm{S_n}(\mathrm{a},\mathrm{b})}{\mathrm{S_i}(\mathrm{a},\mathrm{b})}}\, \mathrm{G}(\mathrm{a},\mathrm{b}) \quad (1)$$

In Eq. (1), the term $\hat{\mathrm{I}}(\mathrm{a},\mathrm{b})$ characterizes the image restoration, the parameter $\mathrm{G}(\mathrm{a},\mathrm{b})$ denotes the degrading input image, $\mathrm{H}(\mathrm{a},\mathrm{b})$ implies the process of degradation, and $\mathrm{H}*(\mathrm{a},\mathrm{b})$ signifies the intricate conjugate, and $\mathrm{S_n}(\mathrm{a},\mathrm{b})$ signifies the power spectral densities of the noise and $\mathrm{S_i}(\mathrm{a},\mathrm{b})$ shows the real image, respectively.

The WF works by estimating local image statistical properties and using that data to adjust its filtering process to minimize noise while preserving the image's structural and textural properties. Thus, when the WF is applied to images of orange fruits, its ability to dynamically adjust to changing image properties will ensure that the fruit's disease-related characteristics, such as lesions, spots, discoloration, and surface abnormalities, remain intact, which are necessary for correct segmentation and feature extraction.

3.2 CLAHE-Based Contrast Enhancement

Contrast enhancement is a pre-processing step used in the proposed framework for the detection of orange fruit diseases to improve disease-affected regions. Images of orange fruits are often subjected to unbalanced lighting conditions and surface reflections, which can obscure disease symptoms. This problem is addressed through the use of CLAHE prior to segmentation. CLAHE increases local contrast through the separation of images into small, non-overlapping tiles. In this study, CLAHE was applied only to the Luminance channel (L) after transforming the image to the lab color space, thus preserving color data. This improves lesion visibility for better segmentation and feature extraction, as shown in Figure 2.

3.3 RGB Threshold - Based Disease Region Segmentation

RGB (red, green, and blue) color thresholding offers numerous advantages for the identifying diseases in orange fruits. These include the ability to differentiate among areas of the fruit that may have changed color due to the presence of a disease. For example, disease can cause dark brown spots, white patches, or even discoloration of the fruit's skin from green to yellow. Thresholding of RGB colors aids in identifying a possible disease location on the fruit by isolating colors indicative of disease. Separated color images indicate the likelihood of a disease being present in certain areas of the fruit. Segmented regionsprovide a wealth of information related to the color distribution, texture, and overall appearance of the segmented regions, which aids in determining the type of disease present on the fruit, as seen in Figure 2.

Additionally, RGB thresholding is relatively simple to program and uses limited computer resources, making it appropriate for real-time applications. RGB thresholding can accommodate changes to the threshold values based on the unique color characteristics of the various diseases affecting orange fruits and/or the lighting conditions that existed during image acquisition, enabling its implementation across multiple datasets.

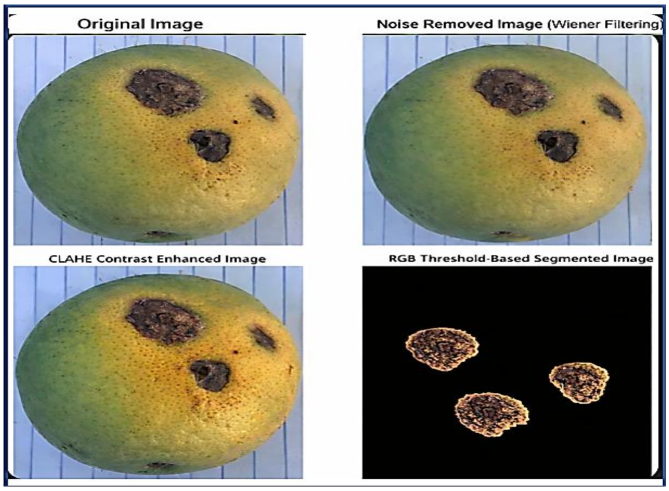

Figure 2. Visual illustration of noise reduction, contrast enhancement, and RGB- threshold-based segmentation on orange fruit images

3.4 Entropy-Based Feature Extraction

In this work, a new method for enhancing the accuracy and robustness of disease detection in orange fruits was developed. This method employs an advanced methodology for fusing deep features extracted from three CNNs: ResNet50, VGG-16, and NASNet. The use of feature fusion in the proposed work is significant, as it provides a method to combine complementary and discriminative feature representations generated by several different deep architectures. The final classification layer of each pre-trained architecture was removed, and the pre-trained CNN models were employed as fixed feature extractors with frozen convolutional layers. Since the convolutional layers were not updated during training, the networks retained their pre-trained weights while extracting deep feature representations from the segmented orange fruit images. The extracted features were subsequently fused using the entropy-based fusion methodology [15]. The ResNet50, VGG-16, and NASNet architectures provided complementary feature representations by capturing texture, color, shape, and structural lesion patterns present in the orange images. The entropy-based feature fusion strategy combined these complementary representations into a unified feature space, resulting in a more comprehensive description of disease characteristics and improving the discriminative capability of the subsequent classifier.

For each segmented orange fruit image, 2048 deep features were extracted from ResNet50, 4096 features from VGG-16, and 4032 features from NASNet. These feature vectors were concatenated to form a high-dimensional feature representation. Because direct concatenation may introduce redundant information and increase computational complexity, the entropy-based fusion approach was employed to preserve the most informative complementary features while reducing redundancy, thereby improving the efficiency and classification performance of the proposed framework.

Therefore, to overcome the aforementioned challenges, an entropy-based feature fusion technique is employed in this research work. The entropy value represents the amount of information contained in each feature; therefore, features exhibiting high-entropy values contain more information and exhibit greater variability than features exhibiting low-entropy values, which typically represent redundant or less informative data. Based on the computed entropy values, the authors allocate adaptive weights to each of the feature subsets to emphasize informative features while minimizing the effect of redundant features. The proposed approach utilizes an integrated representation of the individual deep feature vectors and, therefore, can provide a more robust and informative set of features than would have been generated using any of the individual architectures alone. It is defined as Eqs. (2)-(4):

$$f_{ResNet50_{1\times n}} = \{ResNet50_{1\times 1}, ResNet50_{1\times 2} ResNet50_{1\times 3}, \cdots, ResNet50_{1\times n}\} \tag{2}$$

$$f_{VGG16_{1\times m}} = \{VGG16_{1\times 1}, VGG16_{1\times 2}, VGG16_{1\times 3}, \cdots, VGG16_{1\times m}\} \tag{3}$$

$$f_{NasNet_{1\times l}} = \{NasNet_{1\times 1}, NasNet_{1\times 2}, NasNet_{1\times 3}, \cdots, NasNet_{1\times l}\} \tag{4}$$

The combined feature representation is obtained by fusing the individual feature vectors from each model, as shown in Eq. (5):

$$\text{Fused(features vector)}_{1\times q} = \sum_{i=1}^{3} \{ f_{ResNet50_{1\times n}}, f_{VGG16_{1\times m}}, f_{NasNet_{1\times l}}\} \tag{5}$$

The fused feature vector integrates the features extracted from ResNet50, VGG-16, and NASNet into a single representation for orange fruit disease detection. This combined feature set is further used for classification in the proposed model.

3.5 Hyperparameter Optimization of DCRNN using Enhanced Sea Horse Optimization Algorithm

To obtain the best possible results from the Deep Convolutional Recurrent Neural Network (DCRNN), hyperparameters tuning must be done effectively. For that reason, this research uses the Enhanced Sea Horse Optimization (ESHO) algorithm to automatically define the best hyperparameters for the DCRNN model. The SHO (Sea Horse Optimization) algorithm was enhanced to improve its ability to maintain diversity among the population, increase convergence speed, and offer an improved balance between exploration and exploitation of the search space [16]. The entropy-fused feature vector attained from the ResNet50, VGG16, and NASNet techniques has been reshaped and supplied to the recurrent framework for classification. The sequence length given to the recurrent layer was set to 64, allowing the approach to efficiently acquire contextual dependencies within the extracted feature sequence. The outcome sequence representation is subsequently processed through the attention and classification layers to provide the final disease estimation.

In the ESHO framework, each sea horse signifies a candidate value with respect to a particular hyperparameter set of the DCRNN model, defined as:

$$X_i = [\, \eta_i, k_i, f_i, p_i, h_i, W_i]$$

Where, $\eta_i, k_i, f_i, p_i, h_i$, and W_i represent the learning rate, the convolution size, the count of filters, the pooling size, the count of recurrent (LSTM) units, and the recurrent weight parameter, respectively.

The quality of every candidate value is assessed using a fitness function that minimizes classification error, which is defined as shown in Eq. (6):

$$F(X_i) = 1 - \text{Accuracy}_{DCRNN}(X_i) \tag{6}$$

A lower fitness value indicates better classification performance and guides the optimization process toward optimal hyperparameter configurations.

Position Update

The ESHO algorithm has an exploration, exploitation, and reproduction phase to update the location for each seahorse. These phases include:

- **Exploration Phase (Global Search):** During this phase, the seahorses explore the search space to avoid early convergence. The new location is determined by a random movement from ocean currents that determine direction and speed.

$$X_i^{t+1} = X_i^t + r_1 \cdot (X_{rand}^t - X_i^t) \tag{7}$$

In Eq. (7), where $r_1 \in [0,1]$ is a random number, and X_{rand}^t is a randomly selected sea horse position.

- **Exploitation Phase (Local Refinement):** In the exploitation phase, the sea horses move toward the best solution found in order to better define the most favorable area(s) within the search space, as shown in Eq. (8):

$$X_i^{t+1} = X_i^t + \alpha \cdot (X^* - X_i^t) \tag{8}$$

In Eq. (8), where X^* is the global best solution found, and α is an adaptive convergence coefficient that decreases over iterations to enhance stability.

- **Enhanced Reproduction and Survival Strategy:** To improve the likelihood of finding the optimal solution, the reproduction strategy for ESHO allows weaker sea horses to be eliminated and replaced by newly created offspring located closer to areas of higher fitness, as shown in Eq. (9):

$$X_{new} = X^* + \beta \cdot \mathcal{N}(0,1) \tag{9}$$

In Eq. (9), where $\mathcal{N}(0,1)$ implies Gaussian noise and β denotes the mutation strength

- **Termination Criterion and Optimal Solution:** Optimization will continue until either the maximum number of iterations has been performed or convergence has occurred. The initial hyperparameter values for DCRNN using ESHO. The final solution represents the best DCRNN hyperparameters that were identified during the optimization process:

$$X^* = [\eta^*, k^*, f^*, p^*, h^*, W^*]$$

Optimized hyperparameters for the DCRNN model was found using ESHO, and they have greatly improved classification accuracy and robustness with respect to orange fruit disease detection. The inclusion of ESHO eliminated the need for manually tuning all possible combinations; It also increased convergence to global optima solutions and improved generalization performance. Therefore, this is an ideal optimization strategy for applications related to precision agriculture.

3.6 Classification Section

Using deep feature extraction methods (ResNet50, VGG-16, NASNet) and combining them with an entropy-based feature fusion method, the generated combined feature vector(s) were analyzed by the following three deep learning algorithms: Stacked Sparse Autoencoder (SSAE); multi-head attention-based LSTM (MHA-LSTM); and the presented ESHO-DCRNN method to measure the potential of the combined features in discriminating orange fruit diseases into their respective classes.

3.6.1 Stacked Sparse Auto Encoder (SSAE)

The SSAE is one of the unsupervised DL techniques that applies sparseness constraints on neuron activation values to produce compact and discriminative feature representations [17]. The SSAE is constructed from multiple sparse autoencoder layers stacked one upon another. For an input fused feature vector x, the encoding operation is defined as:

$$h = f(W_x + b) \tag{10}$$

Following layer-wise unsupervised pre-training, a Softmax classifier was added to the top of the SSAE so that it could be trained to perform multiclass classification of orange fruit diseases. The SSAE reduces redundant feature dimensionality, increases class separation, and makes the network more robust to noise.

3.6.2 Multi-Head Attention-based LSTM (MHA-LSTM)

The MHA-LSTM is a combination of the sequential system abilities of LSTM networks and an MHA module to selectively concentrate on which aspects of the deep features are most relevant to the classifier tasks [18].

The internal operations of an LSTM unit are defined as follows:

$$i_t = \sigma(W_i x_t + (U_i h_{t-1}) \tag{11}$$

$$f_t = \sigma(W_f x_t + (U_f h_{t-1}) \tag{12}$$

$$o_t = \sigma(W_o x_t + (U_o h_{t-1}) \tag{13}$$

$$c_t = f_t \odot c_{t-1} + i_t \odot \tanh(W_c x_t) \tag{14}$$

$$h_t = o_t \odot \tanh(c_t) \tag{15}$$

To further improve classification efficiency, an MHA is applied to the LSTM outputs, allowing the model to learn multiple attention distributions over the feature space as shown in Eq. (16):

$$\text{Attention}\ (Q, K, V) = \text{softmax}\ \frac{QK^T}{\sqrt{d_k}} \tag{16}$$

The MHA-LSTM focuses on disease-specific patterns in the images, such as lesions, discoloration, and texture irregularities, while ignoring background information irrelevant to the classification task. The attention-weighted deep features are then entered into the Softmax classifier.

3.6.3 Optimized DCRNN Classifier (ESHO-DCRNN)

Incorporating recurrent learning with deep convolutional encoding, the DCRNN addresses the limitations of prior works through its ability to learn hierarchical abstractions of disease image features and their contextual dependencies. Hierarchical abstractions are obtained through the convolutional component of the network. Contextual dependencies are modeled through the recurrent components of the network. The DCRNN incorporates three stacked recurrent layers with ReLU activation functions. Each of these recurrent layers produces a transformed version of the input that includes information about the input data sequence up to that point. Fully connected layers follow each of these recurrent layers, providing a progressive refinement of the learned representation [19]. Finally, a Softmax output layer performs the final classification on the refined representation to determine which of the available classes the input corresponds to. The complete structure of the DCRNN method is exhibited in Figure 3.

By combining deep feature representations with a layer-wise optimized DCRNN classifier, the proposed system effectively captures the intricate spatio-temporal patterns present in orange fruit disease images. The use of recurrent layers with ReLU activation, fully connected transformation, and Softmax-based decision-making provides robust multi-class classification performance. Therefore, the DCRNN model demonstrates a high degree of model performance and excellent robustness, making it suitable for application in automated orange fruit disease detection in precision agriculture.

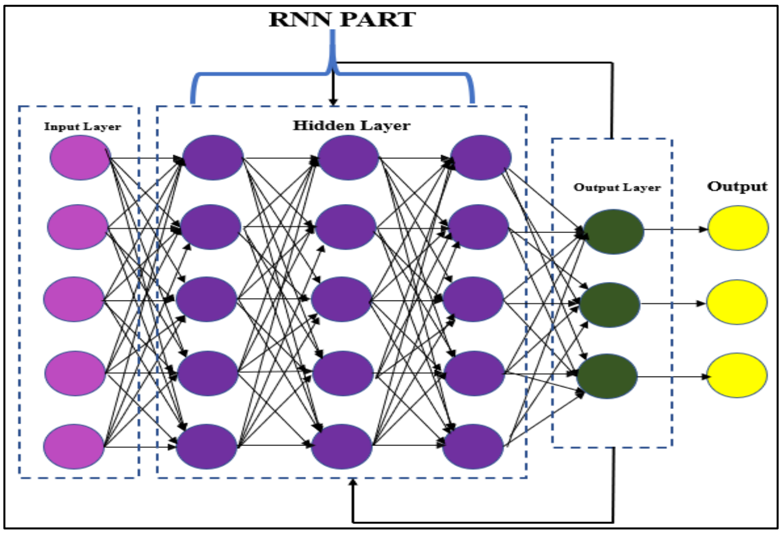

Figure 3. Structure of DCRNN

3.6.4 Classifier Comparison

All three classifiers, SSAE, MHA-LSTM, and ESHO-Optimized DCRNN, are compared using the same fused deep feature set in order to provide an equal basis of comparison. The performance of every classifier is assessed by comparing its accuracy, precision, recall, specificity, and F1-score. The experimentatal outcomes show that the ESHO-

Optimized DCRNN realizes the highest classification performance and superior generalization for orange disease detection and multiclass classification.

4. Experimental Results

4.1 Implementation Setup

The method runs on Python 3.6.5 with an i5-8600k CPU, 4GB GPU, 16GB RAM, 250GB SSD, and 1TB HDD. The proposed ESHO-DCRNN method achieves high levels of accurate detection and classification of orange fruits. Experiments were performed using images of healthy and diseased orange fruits. Each experiment was performed by utilizing a computer system. The classification capabilities of the ESHO-DCRNN were evaluated by assessing its performance using a commonly accepted performance evaluation, which provides an assessment of the ESHO-DCRNN's ability to differentiate among various categories of orange fruit diseases. A portion of the images provided within the Orange_Fruit dataset, which was acquired from the Kaggle database [20], included 3000 images of citrus cankers, 3000 images of healthy oranges, and 2600 images of melanose infections. Since the dataset had a class imbalance issue, as there were fewer melanose images than the other two categories, a dataset balancing technique was applied. A total of 2600 images were randomly sampled from both the citrus canker and healthy image classes, and these images were then added to create a new balanced dataset containing 2600 images per class. The application of this dataset balancing technique reduced bias toward the majority classes present in the dataset and improved the ability of the ESHO-DCRNN to generalize to the conditions represented by the images in the dataset. Images representing each of the three disease categories and some of their visual features are presented in Figure 4 and Table 1, showing that the dataset contains three classes with a total of 7,800 samples. Table 2 shows the parameter settings of the proposed model.

Table 1. Dataset details

Class	No. of. Instances
Citrus canker	2600
Healthy	2600
Melanose	2600
Total	7800

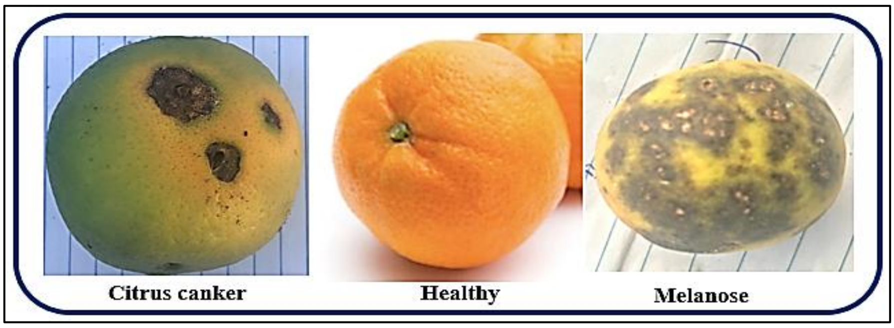

Figure 4. Sample images

Table 2. Parameter setting for ESHO-DCRNN

Models	Parameters	Values
Preprocessing (Wiener Filter)	Filter Kernel Size	5×5
	Noise Variance	0.05

CLAHE Enhancement	Clip Limit	3.0
	Tile Grid Size	8×8
Color-Based Segmentation	RGB Threshold Range	80–180
	Segmentation Threshold	0.5
ResNet50 Feature Extractor	Feature Dimension	2048
	Dropout Rate	0.2
VGG-16 Feature Extractor	Feature Dimension	4096
	Fine-Tuned Layers	Last 4
NasNet Feature Extractor	Feature Dimension	4032
	Dropout Rate	0.2
Entropy-Based Fusion	Fusion Method	Entropy Fusion
	Fusion Dimension	512
	Entropy value of ResNet50	0.71
	Normalized weight of ResNet50	0.38
	Entropy value of VGG16	0.80
	Normalized weight of VGG16	0.34
	Entropy value of NASNetMobile	0.92
	Normalized weight of NASNetMobile	0.28
SSAE Classifier	Hidden Layers	3
	Hidden Units	128
	Latent Dimension	64
	Sparsity Weight	0.001
MHA-LSTM Classifier	LSTM Units	128
	Attention Heads	4
	Number of Layers	2
	Dropout Rate	0.2
DCRNN Classifier	Graph Convolution Units	128
	Recurrent Units	128
	Number of DCRNN Layers	3
	Dropout Rate	0.2
Enhanced Sea Horse Optimization (ESHO)	Population Size	30
	Maximum Iterations	100
	Exploration Coefficient	0.5
	Exploitation Coefficient	0.5
Training Configuration	Optimizer	AdamW
	Learning Rate	0.001
	Batch Size	32
	Epochs	50

4.2 Discussions and Observations

As shown in Table 3, a comparative assessment was performed among the three classifications used for evaluating performance: the SSAE, the MHA-LSTM, and the proposed ESHO-DCRNN. Using the common evaluation parameters of $accur_y$, $preci_n$, $speci_y$ $sensi_y$, and F_{score}, the proposed ESHO-DCRNN exhibited the greatest classification performance; it obtained an $accur_y$ of 99.50% and also had a $preci_n$ of 99.37%, a $sensi_y$ of 99.27%, a $speci_y$ of 99.67%, and an F_{score} of 99.32%. The MHA-LSTM classifier achieved an $accur_y$ of 99.10% and an F_{score} of 98.95%, whereas the SSAE classifier obtained the lowest performance with an $accur_y$ of 99.00% and an F_{score} of 98.77%. The improved performance of the proposed ESHO-DCRNN is due to the successful combination of the deep convolutional and recurrent learning architectures and the optimum selection of hyperparameters through the use of the Enhanced Sea Horse Optimization (ESHO). The above results demonstrate the robustness, ability to discriminate, and superior generalized performance of the ESHO-DCRNN method for correct identification and categorization of orange fruit diseases.

Table 3. Classification performance of SSAE, MHA-LSTM, and ESHO-DCRNN

Classifier	$Accur_y$(%)	$Preci_n$(%)	$Speci_y$ (%)	$Sensi_y$ (%)	F_{score}(%)
SSAE	99.00	98.85	99.20	98.70	98.77
MHA-LSTM	99.10	99.00	99.30	98.90	98.95
Proposed ESHO-DCRNN	99.50	99.37	99.67	99.27	99.32

Figure 5 displays the performance of the proposed ESHO-DCRNN model over 50 epochs for both training and testing. These two plots illustrate how the accuracy and loss functions vary as the learning process continues. Both the training and testing accuracy plots display a continuous upward trend at an extremely high rate, illustrating that features are being learned efficiently and that there is strong convergence. Accuracy during the training phase improves from roughly 95.20% at epoch 10 to nearly 99.40% by epoch 50. Similarly, the testing accuracy also shows a comparable improvement during this time frame, going from nearly 96.10% to 99.50%, which illustrates that the model generalizes very well and does not exhibit significant overfitting. The plots for training and testing loss are shown on the right side of Figure 5. Both loss plots steadily decrease throughout the training and testing phases of the model's development. The training loss decreases from roughly 0.28 to 0.12, and the testing loss decreases from roughly 0.32 to 0.14. The fact that the training and testing loss plots are so close to one another indicates that the learning process was stable and that the Enhanced Sea Horse Optimization (ESHO) method effectively tuned the parameters of the DCRNN model. In total, the results illustrated in Figure 5 indicate that the proposed ESHO-DCRNN model will be able to classify diseases of orange fruits accurately and efficiently.

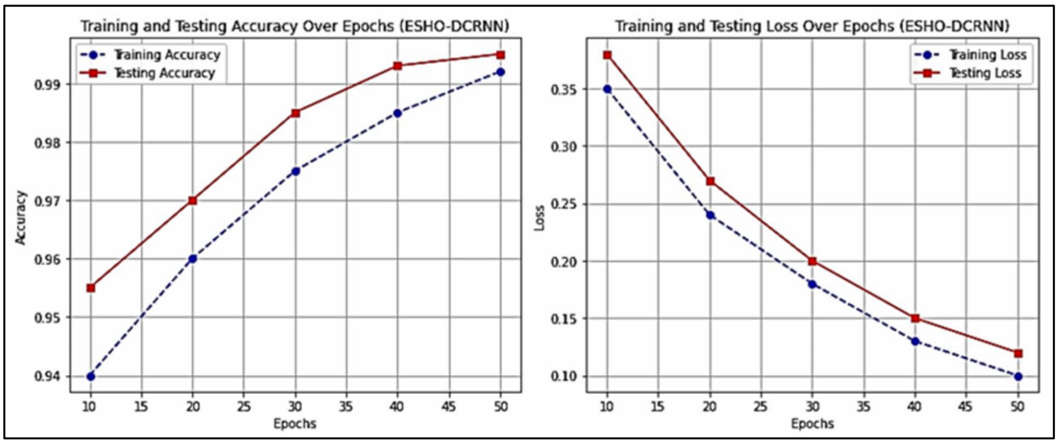

Figure 5. Accuracy & loss graph based on training and testing data of the proposed ESHO-DCRNN classifier over 50 epochs

Figure 6 reveals the classifier results of the ESHO-DCRNN approach with a 70:30 train/test split. The confusion matrices shown in subfigures (a) and (b) provide evidence that the model has high classification accuracy, as it correctly classifies the samples into their respective disease categories. Finally, the AUC values from the ROC curves in subfigure (d) further validate the superior discriminatory ability of the model.

Table 4 summarizes the performance of the proposed ESHO-DCRNN on the classification task during both the training (70%), testing (30%) phases across three classesCitrus Canker, Healthy, and Melanose. During the training phase, the ESHO-DCRNN model achieved an average overall accuracy of 99.27%, with 99.13% precision, 99.47% specificity, 99.03% sensitivity, and an F1-score of 99.08%. These results indicate a successful and stable training process with extremely low misclassification error rates across all classes.

The testing results demonstrate consistent improvement over the training results, with the model achieving an average accuracy of 99.50%, 99.37% precision, 99.67% specificity, 99.27% sensitivity, and a 99.32% F1-score. Notably, the testing results show slight improvements over the training results in terms of accuracy and specificity, which demonstrates a high level of generalization and robustness by the ESHO-DCRNN model. The results of this study demonstrate the ability of the proposed method to successfully discriminate between images of healthy oranges and oranges suffering from diseases, and to maintain high levels of reliability when used to classify unknown data. Therefore, the proposed ESHO-DCRNN method is well-suited for use in real-world agricultural disease detection systems.

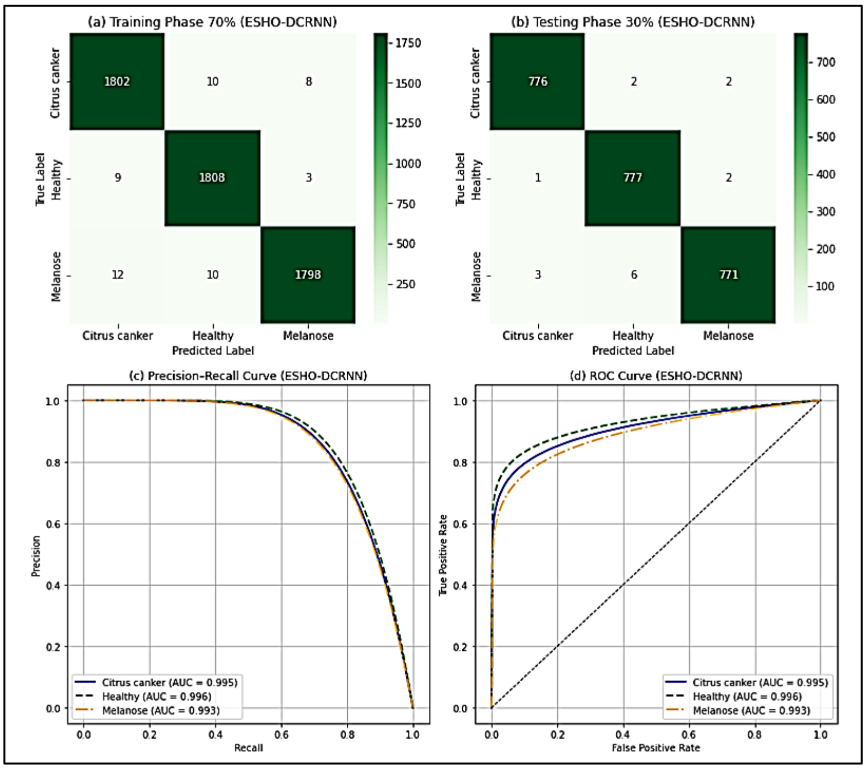

Figure 6. Classifier result of the ESHO-DCRNN method with (a-b) Confusion matrices and (c-d) curves of PR and ROC for 70:30

Table 4. Overall outcomes of the proposed ESHO-DCRNN model for orange fruit disease detection and classification

Training Phase (70%)					
Class	**Accuracy (%)**	**Precision (%)**	**Specificity (%)**	**Sensitivity (%)**	**F1-score (%)**
Citrus canker	99.20	99.10	99.40	99.00	99.05
Healthy	99.60	99.50	99.80	99.40	99.45
Melanose	99.00	98.80	99.20	98.70	98.75
Average	99.27	99.13	99.47	99.03	99.08
Testing Phase (30%)					
Class	**Accuracy (%)**	**Precision (%)**	**Specificity (%)**	**Sensitivity (%)**	**F1-score (%)**
Citrus canker	99.60	99.50	99.80	99.40	99.45
Healthy	99.80	99.70	99.90	99.60	99.65
Melanose	99.10	98.90	99.30	98.80	98.85
Average	99.50	99.37	99.67	99.27	99.32

Table 5 shows the cross-validation (Five-fold) results of the ESHO-DCRNN method, which provides evidence for a high degree of consistency and dependability of the system. The outcome suggests stable and greater performance across all folds, with a mean $accur_y$ of 99.50% ± 0.04%, demonstrating the strong generalization capability of the proposed model.

Table 5. Five-fold evaluation metrics demonstrating the consistency of the ESHO-DCRNN model's performance

Fold No.	$Accur_y$ (%)	$Preci_n$ (%)	$Sensi_y$ (%)	F_{score} (%)
Fold 1	99.44	99.48	99.36	99.42
Fold 2	99.48	99.53	99.39	99.46
Fold 3	99.55	99.60	99.45	99.52
Fold 4	99.50	99.56	99.42	99.49
Fold 5	99.52	99.58	99.44	99.51
Mean ± SD	99.50 ± 0.04	99.55 ± 0.04	99.41 ± 0.03	99.48 ± 0.04

Table 6 presents the comparative study of the ESHO-DCRNN method under the Orange_Fruit Dataset [21] with other methodologies using evaluation metrics. The result implied that the AlexNet, VGG-16, GoogLeNet, ResNet, and DenseNet [22] methods have performed worse outcomes, while the VGG-16-CNN [23] approach has got slightly higher outcome with $accur_y$ of 93.66% and an F_{score} of 93.25%. At the same time, the proposed ESHO-DCRNN approach has achieved maximal value with $accur_y$ of 99.50%, $sensi_y$ of 99.27%, $preci_n$ of 99.37%, and F_{score} of 99.32%. The higher outcome of the proposed ESHO-DCRNN technique can be attributed to the complementary class of multi-CNN feature fusion and an adaptive parameter optimizer. Unlike traditional CNN methods, it captures both spatial and sequential patterns, helping distinguish similar disease classes more effectively. However, performance may vary in real-world conditions due to noise and domain shifts.

Table 6. Comparative result of the ESHO-DCRNN method with existing models under Orange_Fruit Dataset

Model	$Accur_y$ (%)	$Sensi_y$ (%)	$Preci_n$ (%)	F_{score} (%)
AlexNet [22]	88.18	87.40	87.90	87.65
VGG-16[22]	90.47	89.80	90.10	89.95
GoogleNet [22]	91.73	91.10	91.40	91.25
ResNet [22]	91.85	91.30	91.60	91.45
DenseNet [22]	92.46	91.0	92.20	92.05
VGG-16-CNN [23]	93.66	93.10	93.40	93.25
Proposed ESHO-DCRNN	99.50	99.27	99.37	99.32

Table 7 illustrates the comparative study of the ESHO-DCRNN method with other methodologies under the orange diseases dataset [24]. The result implied that the KNN, Random Forest, Naïve Bayes, Logistic Regression, and VGG16 methods have performed worse outcomes, while the ResNet50 approach has got slightly higher outcome with $accur_y$ of 89.67% and an $F1_{score}$ of 88.38%. At the same time, the proposed ESHO-DCRNN approach has achieved maximal value with $accur_y$ of 96.82%, $Reca_{ll}$ of 96.55%, $preci_n$ of 96.55%, and $F1_{score}$ of 96.55%.

Table 7. Comparative result of the ESHO-DCRNN method with existing models under orange diseases dataset

Classifier	Accuracy	Recall	Precision	F1 Score
KNN	72.50	75.30	83.30	79.10
Random Forest	70.00	74.20	84.40	78.97
Naïve Bayes	80.00	78.90	80.60	79.74
Logistic Regression	85.00	86.60	87.00	86.80
VGG16	87.50	87.50	92.36	89.86
ResNet50	89.67	88.34	88.43	88.38
ESHO-DCRNN	96.82	96.55	96.55	96.55

Table 8 shows the computational efficiency of the ESHO-DCRNN model compared to other techniques [25]. The pretrained ResNet50, VGG16, and NASNetMobile networks were utilized solely for feature extraction. Consequently, the parameter count reported for ESHO-DCRNN reflects the trainable complexity of the entropy-based fusion and DCRNN classification modules rather than the cumulative parameters of all pretrained backbone networks. Based on inference time, the ESHO-DCRNN method provides a lower value of 3.18ms, FLOPs of 6728945G, and Params of 58.22M whereas the ResNET50, Resnet34, ResNET18, VGG16, AlexNet, EfficientNet_b0 and NCNN-FLD techniques attain higher time of 6.36ms, 8.32ms, 7.46ms, 4.30ms, 8.22ms, 8.49ms, and 7.95, respectively.

Table 8. Computational efficiency of the ESHO-DCRNN method

Models	FLOPs (G)	Params (M)	Inference Time (ms)
ResNET50	7647974656	25557032	6.36
Resnet34	6843157120	21797672	8.32
ResNET18	3399159296	11689512	7.46
VGG16	27235905024	138357544	4.30
AlexNet	1201895168	61100840	8.22
EfficientNet_b0	746469072	5288548	8.49
NCNN-FLD	335157314	172.314	7.95
ESHO-DCRNN	6728945	58.22	3.18

Table 9 indicates the ablation study of the proposed ESHO-DCRNN methodology under Orange-Fruit Dataset. The ResNet50 + DCRNN, attains an $accu_y$ of 97.14%, $prec_n$ of 96.82%, $reca_l$ of 96.91%, and $F1_{score}$ of 96.86%. and ResNet50 + VGG16 + DCRNN providing an $accu_y$ of 98.03%, $prec_n$ of 97.76%, $reca_l$ of 97.84%, and $F1_{score}$ of 97.80%. Additionally, the Entropy Fusion + DCRNN attained a better $accu_y$ to 98.67%, $prec_n$ to 98.45%, $reca_l$ to 98.53%, and $F1_{score}$ to 98.49%. Moreover, the Entropy Fusion + ESHO-DCRNN, additionally increased $accu_y$ to 99.12%, $prec_n$ to 99.01%, $reca_l$ to 99.08%, and $F1_{score}$ to 99.04%. Meanwhile, the Proposed ESHO-DCRNN model, achieved the maximum outputs performance, $accu_y$ of 99.50%, $prec_n$ of 99.27%, $reca_l$ of 99.37%, and $F1_{score}$ of 99.32%, emphasising the efficiency of the components.

Table 9. Ablation study of the ESHO-DCRNN method under orange-fruit dataset

Model	Accuracy	Precision	Recall	F1-Score
ResNet50 + DCRNN	97.14	96.82	96.91	96.86
ResNet50 + VGG16 + DCRNN	98.03	97.76	97.84	97.80
Entropy Fusion + DCRNN	98.67	98.45	98.53	98.49
Entropy Fusion + ESHO-DCRNN	99.12	99.01	99.08	99.04
Proposed ESHO-DCRNN	99.50	99.27	99.37	99.32

Table 10 demonstrates the ablation study of the presented ESHO-DCRNN architecture under Orange-Disease Dataset. The ResNet50 + DCRNN, got lowest performance, $accu_y$ of 93.64%, $prec_n$ of 93.22%, $reca_l$ of 93.18%, and $F1_{score}$ of 93.20%. and ResNet50 + VGG16 + DCRNN providing better $accu_y$ of 94.42%, $prec_n$ of 94.11%, $reca_l$ of 94.08%, and $F1_{score}$ of 94.09%. Additionally, the Entropy Fusion + DCRNN, achieves a slightly higher $accu_y$ to 95.36%, $prec_n$ to 95.14%, $reca_l$ to 95.10%, and $F1_{score}$ to 95.12%. Moreover, the Entropy Fusion + ESHO-DCRNN, additionally enhanced $accu_y$ to 96.21%, $prec_n$ to 96.02%, $reca_l$ to 96.01%, and $F1_{score}$ to 96.01%. Meanwhile, the Proposed ESHO-DCRNN model, achieved the higher performance, $accu_y$ of 96.82%, $prec_n$ of 96.55%, $reca_l$ of 96.55%, and $F1_{score}$ of 96.55%, states the proficiency of the individual and combined components of the proposed model.

Table 10. Ablation study of the ESHO-DCRNN method under the orange-disease dataset

Model	Accuracy	Precision	Recall	F1-Score
ResNet50 + DCRNN	93.64	93.22	93.18	93.20
ResNet50 + VGG16 + DCRNN	94.42	94.11	94.08	94.09
Entropy Fusion + DCRNN	95.36	95.14	95.10	95.12
Entropy Fusion + ESHO-DCRNN	96.21	96.02	96.01	96.01
Proposed ESHO-DCRNN	96.82	96.55	96.55	96.55

Figure 7 displays the Grad-CAM visualizations generated by the proposed ESHO-DCRNN architecture for representative orange disease samples. The heatmaps indicate that the model predominantly focuses on only affected regions, comprising discolored, necrotic, and damaged tissue areas related to orange diseases. The red and yellow regions show high activation levels, specifying a stronger influence on the model's estimation, whereas blue regions are related to areas with the least contribution. These outcomes illustrate that the presented methodology effectively learns disease-relevant visual patterns rather than depending on background information, thus improving the interpretability, transparency, and reliability of the classification process. The Grad-CAM analysis further ensures that the model's decisions are primarily based on the clinically relevant disease manifestations that exist on the fruit surface.

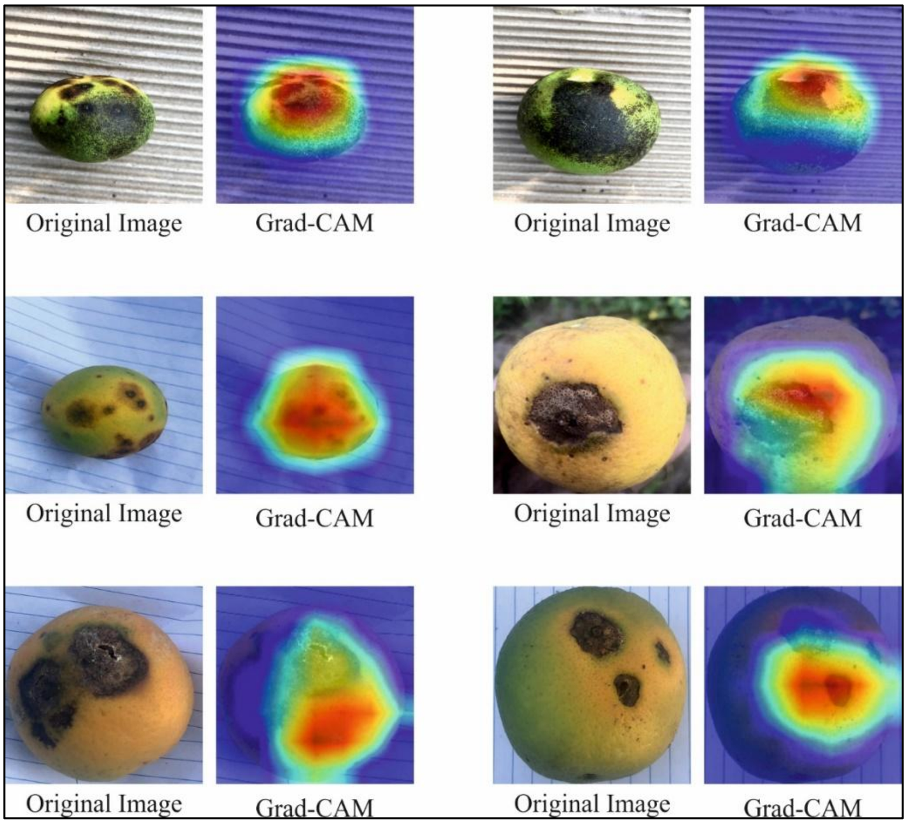

Figure 7. Grad-CAM visualizations of representative orange disease samples

The presented architecture could be incorporated into current agricultural workflows by mobile phone-based applications, field imaging technology, drone-driven monitoring platforms, or a cloud-enabled smart farming environment. In a real-time deployment, orange fruit images acquired in orchards are first subjected to the presented preprocessing flow and subsequently analyzed by the tuned ESHO-optimized multi-feature fusion architecture. The outcome of disease classification could be communicated to farmers or agricultural specialists through user-friendly interfaces, allowing for early disease detection and timely intervention.

This incorporation could help with constant orchard surveillance, decrease crop losses, and enhance disease management effectiveness. Therefore, the presented architecture offers a better foundation for the growth of a smart decision-support network for practical orange disease management. Moreover, the presented architecture has the potential to offer economic advantages through early disease detection, decreasing the effort related to manual orchard inspection, and reducing crop losses, thus contributing to enhanced fruit quality and agricultural productivity.

5. Conclusion and Future Work

The ESHO-DCRNN is an advanced deep learning framework designed for the automatic identification and classification of diseases in orange fruits. It integrates a deep CNN for spatial feature extraction and an RNN for contextual relationships, employing Enhanced Sea Horse Optimization to optimize parameter values and enhance classification accuracy. The model accurately differentiates between healthy oranges and various diseases, achieving a classification accuracy of 99.50%. While it offers improved performance over traditional models, it lacks information on farm origins of datasets and has not explored model compression techniques. Future research aims to create a lightweight version for resource-constrained environments, expand to severity classification, and validate performance across diverse agricultural conditions using edge devices. Enhancements will include disease severity estimation and methods for adapting to new disease patterns without complete retraining.

Declarations

Data Availability Statement

The data that support the findings of this study are openly available in Kaggle repository at https://www.kaggle.com/datasets/sgandhi2003/orange-fruit-dataset and https://www.kaggle.com/datasets/jonathansilva2020/orange-diseases-dataset/data, reference number [20, 21].

Conflict of Interest

The authors declare that they have no known competing financial interests or personal relationships that could have appeared to influence the work reported in this manuscript. All authors contributed to the manuscript and approved the final version.

References

[1] Ayobami, I. O., Oluwabusayo, I., & Olajide A. O. (2019). Classification and Detection of Citrus Disease using Feature Extraction and Support Vector Machine (SVM). International Journal of Computer Applications, 177(17), 17–25. https://doi.org/10.5120/ijca2019919582

[2] Farooq, Muhammad Shoaib, and Abdullah Mehboob. "Prediction of Citrus Diseases Using Machine Learning and Deep Learning: Classifier, Models SLR." arXiv preprint arXiv:2306.01816 (2023).

[3] Sharif, Muhammad, Muhammad Attique Khan, Zahid Iqbal, Muhammad Faisal Azam, M. Ikram Ullah Lali, and Muhammad Younus Javed. "Detection and Classification of

Citrus Diseases in Agriculture Based on Optimized Weighted Segmentation and Feature Selection." Computers and electronics in agriculture 150 (2018): 220-234.

[4] Kaur, Gurjot, Neha Sharma, Sonal Malhotra, Swati Devliyal, and Bura Vijay Kumar. "Citrus Leaf Disease Classification Using VGG16 Convolutional Neural Network Architecture." In 2024 IEEE 9th International Conference for Convergence in Technology (I2CT), IEEE, 2024, 1-6.

[5] Tanwar, Vishesh, Vatsala Anand, Priyanshi Aggarwal, and Mukesh Kumar. "Demonstration of a Highly Developed CNN-SVM Model to Accurately Assess the Degree of Brown Rot in Orange Leaf." In 2024 Fourth International Conference on Advances in Electrical, Computing, Communication and Sustainable Technologies (ICAECT), IEEE, 2024, 1-6.

[6] Kumar, Sandeep, Abhay Kumar Pandey, Daksh Raghav, Gaurav Gupta, and Varsha Srivastava. "A Deep Learning Approach for Multiclass Orange Disease Classification." In 2024 2nd international conference on disruptive technologies (ICDT), IEEE, 2024, 184-189.

[7] PB, KH. "Revolutionizing citrus health: AI-Based Detection of Greening Disease and Nutrient Deficiencies in Sweet Orange." JOURNAL OF EXPERIMENTAL AGRICULTURE INTERNATIONAL Учредители: Sciencedomain International 47, no. 1 (2025): 381-391.

[8] Sghir, A., Mohammed Ziani, and K. El Handri. "A Data-Driven Fusion of Deep Learning and Transfer Learning for Orange Disease Classification." MATHEMATICAL MODELING AND COMPUTING, Vol. 11, No. 3, (2024). 870–882

[9] Suryavanshi, Ankita, Vinay Kukreja, Ayush Dogra, and Lisa Gopal. "Multi-Level Citrus Greening Disease Recognition in Oranges using CNN and Random Forest." In 2023 IEEE Pune Section International Conference (PuneCon), IEEE, 2023, 1-6.

[10] Chauhan, Shanvi. "Leveraging MobileNetV2 for Accurate Detection and Classification of Orange Diseases: A Study on Blackspot, Canker, And Greening Citrus." In 2024 Global Conference on Communications and Information Technologies (GCCIT), IEEE, 2024, 1-6.

[11] Kaur, Arshleen, Vinay Kukreja, Deepak Upadhyay, Manisha Aeri, and Rishabh Sharma. "DeepCitrus: Leveraging Integrated CNN and VGG16 for Automated Orange Leaf Disease Detection." In 2024 IEEE International Conference on Interdisciplinary Approaches in Technology and Management for Social Innovation (IATMSI), vol. 2, IEEE, 2024, 1-5.

[12] Yadav, Pappu Kumar, Thomas Burks, Jianwei Qin, Moon Kim, Quentin Frederick, Megan M. Dewdney, and Mark A. Ritenour. "Citrus Disease Classification with Convolution Neural Network Generated Features and Machine Learning Classifiers on Hyperspectral Image Data." In Autonomous Air and Ground Sensing Systems for Agricultural Optimization and Phenotyping VIII, vol. 12539, SPIE, 2023, 1253902.

[13] Kalaivani, A., and J. Sathya. "Advanced Citrus Disease Analysis: Integrating ML and DL for Improved Identification and Classification." In 2024 International Conference on

Smart Systems for Electrical, Electronics, Communication and Computer Engineering (ICSSEECC), IEEE, 2024, 117-121.

[14] Behera, Santi Kumari, Lipsarani Jena, Amiya Kumar Rath, and Prabira Kumar Sethy. "Disease Classification and Grading of Orange Using Machine Learning and Fuzzy Logic." In 2018 International Conference on Communication and Signal Processing (ICCSP), IEEE, 2018, 0678-0682.

[15] Vidyasri, S., and S. Saravanan. "Enhanced Deep Transfer Learning with Multi-Feature Fusion for Lung Disease Detection." Multimedia Tools and Applications 83, no. 19 (2024): 56321-56345.

[16] Zhao, Shijie, Tianran Zhang, Shilin Ma, and Mengchen Wang. "Sea-Horse Optimizer: A Novel Nature-Inspired Meta-Heuristic for Global Optimization Problems: Sea-Horse Optimizer: A Novel Nature-Inspired Meta-Heuristic for Global Optimization Problems." Applied Intelligence 53, no. 10 (2023): 11833-11860.

[17] Guo, Jiao, Henghui Li, Jifeng Ning, Wenting Han, Weitao Zhang, and Zheng-Shu Zhou. "Feature Dimension Reduction Using Stacked Sparse Auto-Encoders for Crop Classification with Multi-Temporal, Quad-Pol SAR Data." Remote Sensing 12, no. 2 (2020): 321.

[18] Anandhi, D. Felicia Rose, and S. Sathiamoorthy. "Enhancing Rice Plant Disease Recognition and Classification Using Modified Sand Cat Swarm Optimization with Deep Learning." Int. J. Recent Innov. Trends Comput. Commun 11 (2023): 248-256.

[19] Vidyasri, S., and S. Saravanan. "Computer-Aided Diagnosis Model for Lung Diseases Using Sea Lion Optimization with Deep Convolutional Recurrent Neural Network on Chest X-ray Images." International Journal of Engineering Trends and Technology 71 (2023): 60-70.

[20] https://www.kaggle.com/datasets/sgandhi2003/orange-fruit-dataset

[21] https://www.kaggle.com/datasets/jonathansilva2020/orange-diseases-dataset/data

[22] Cai, Chuang, Guoxiong Zhou, and Chao Lu. "Citrus Surface Defect Identification Based on PCS-2D-Otsu and CGWO-DT-SVM." Multimedia Tools and Applications 83, no. 15 (2024): 43649-43672.

[23] Kujur, Lawrence, Varuna Gupta, and Abhinav Singhal. "A Hybrid Multi-Optimizer Approach Using CNN and GB for Accurate Prediction of Citrus Fruit Diseases." Discover Applied Sciences 7, no. 3 (2025): 151.

[24] Nosiba Arifin, Khandoker, Sayma Akter Rupa, Md Musfique Anwar, and Israt Jahan. "Lemon and Orange Disease Classification Using CNN-Extracted Features and Machine Learning Classifier." In Proceedings of the 3rd International Conference on Computing Advancements, 2024, 154-161.

[25] Anwar, Dalya. "A Novel CNN Model for Fruit Leaf Disease Detection: A Lightweight Solution for Grapes, Figs, and Oranges." Fusion: Practice & Applications 19, no. 2 (2024).